ACS APPLIED MATERIALS & INTERFACES

Research Article

www.acsami.org

Mechanism of Polysulfone-Based Anion Exchange Membranes Degradation in Vanadium Flow Battery

Zhizhang Yuan,[†,§] Xianfeng Li,[*,†,‡] Yuyue Zhao,[†,§] and Huamin Zhang[*,†,‡]

[†]Division of Energy Storage, Dalian Institute of Chemical Physics, Chinese Academy of Sciences, 457 Zhongshan Road, Dalian 116023, P. R. China

[‡]Collaborative Innovation Center of Chemistry for Energy Materials (iChEM), Dalian 116023, P. R. China

[§]Graduate School of Chinese Academy of Sciences, Beijing 100039, P. R. China

Supporting Information

ABSTRACT: The stability of hydrocarbon ion exchange membranes is one of the critical issues for a flow battery. However, the degradation mechanism of ion exchange membranes has been rarely investigated especially for anion exchange membranes. Here, the degradation mechanism of polysulfone based anion exchange membranes, carrying pyridine ion exchange groups, under vanadium flow battery (VFB) medium was investigated in detail. We find that sp^2 hybrid orbital interactions between pyridinic-nitrogen in 4,4′-bipyridine and benzylic carbon disrupt the charge state balance of pristine chloromethylated polysulfone. This difference in electronegativity inversely induces an electrophilic carbon center in the benzene ring, which can be attacked by the lone pair electron on the vanadium(V) oxygen species, further leading to the degradation of polymer backbone, while leaving the 4,4′-bipyridine ion exchange groups stable. This work represents a step toward design and construction of alternative type of chemically stable hydrocarbon ion exchange membranes for VFB.

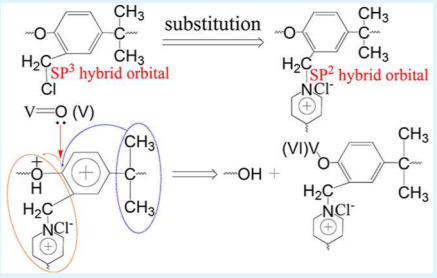

KEYWORDS: *degradation mechanism, polysulfone, 4,4′-bipyridine, hybrid orbital, anion exchange membranes, vanadium flow battery*

INTRODUCTION

The increasing world energy production is highly driven by increasing consumption of fossil fuel resources, which results in critical global environmental concerns and energy shortage.[1] The exploration and development of energy storage, especially large scale energy storage, that can be coupled with renewable energy sources like solar and wind power, are in high demand to address these problems.[2,3] One of the most promising candidates for large scale energy storage is the vanadium flow battery (VFB),[4−6] which was proposed by Skyllaskazacos et al. in the 1980s, due to its attractive features like long cycle life, high efficiency, and high safety. A VFB consists of two tanks filled with active species of vanadium ions in different valence states, two pumps, and a battery cell. The VFB development highly relies on a high-quality membrane, due to the high cost and low selectivity of currently used membranes.[7,8] In a VFB, a membrane plays the role of preventing cross mixing of the positive and negative electrolytes, while transporting protons to complete the circuit. An ideal membrane used in a VFB should meet the requirements of good ion conductivity, high ion selectively, and good chemical stability.[6] Typically, perfluorinated membranes such as Nafion are most commonly used in VFBs as they show excellent electrochemical properties and chemical stability. However, their further applications in VFB have been hampered by their extremely high cost and low ion selectively. Therefore, more and more effort has been devoted to the development of aromatic hydrocarbon based membranes such as sulfonated poly(ether ether ketone) (SPEEK), quaternarized poly(tetramethydiphenyl ether sulfone) (QAPES), and chloromethylated/quaternized poly(phthalazinone ether ketone), due to their high ion selectivity and low cost.[9−13] However, aromatic hydrocarbon membranes normally exhibited poor chemical stability in the strong oxidized VO_2^+ and acidic medium.[14]

Anion exchange membranes (AEMs) have attracted wide attention in both battery systems and alkaline fuel cells. Compared with cation exchange membranes, the anion exchange membranes showed much higher selectivity due to the Donnan exclusion between the positively charged anion exchange groups and vanadium ions. A variety of alkaline exchange membranes (AEMs) based on polysulfones, polyphenylenes, polystyrenes, polyethylenes, poly(arylene ether ketone)s, and poly(phenylene oxide)s have been well studied in the application of flow batteries and fuel cells.[15−17] However, one of the major concerns of AEMs is their low chemical stability under battery operating conditions.

Until now, a number of studies exemplify the degradation mechanism of anion exchange membranes (AEMs) in alkaline fuel cell systems.[18−20] Quantum mechanics calculations combined with experimental verification have demonstrated

Received: June 30, 2015
Accepted: August 18, 2015
Published: August 18, 2015

DOI: 10.1021/acsami.5b05840
ACS Appl. Mater. Interfaces 2015, 7, 19446−19454

that the primary AEM degradation involves hydroxide ions, a potent nucleophile, attack on the fixed cation groups of AEMs, leading to direct nucleophile substitution, Hoffman elimination, and chemical rearrangements induced through ylide intermediate formation.[17,21,22] However, there are very rare reports on the degradation mechanism of the hydrocarbon anion exchanged membranes under acidic VFB medium, which leads to few relevant strategies for synthesizing new materials with excellent chemical stability for VFB application. Accordingly, it is urgent to clarify the degradation mechanism of non-fluorinated anion exchange membranes, which will be highly beneficial to exploring high-performance VFB membranes.

Recently, we reported an anion exchange membrane with internal cross-linking networks for a vanadium flow battery.[23] The internal cross-linking networks, constructed by reacting 4,4′-bipyridine with chloromethylated polysulfone, ensure the membranes with excellent stability, showing very promising performance (continuously running more than 1600 cycles) for vanadium flow battery application. Considering the durability of energy storage systems (long calendar life (e.g., >15 years) and long cycle life (e.g., >4000 deep cycles for energy applications)), the chemical stability of the membranes is still inadequate to meet the long-term flow battery systems, which is of paramount importance for practical use.[5,24] In this paper, the degradation mechanism of polysulfone based anion exchange membranes will be first investigated and clarified.

EXPERIMENTAL SECTION

Chloromethylation of Polysulfone. The chloromethylated polysulfone (CMSPF) polymer was prepared through a common chloromethylation method.[25] 15 g of polysulfone (PSF Udel-3500) was dissolved in 600 mL of chloroform in a three-necked round-bottomed flask. A volume of 1.2 mL of anhydrous $SnCl_4$ was slowly added into the polymer solution under a nitrogen atmosphere and stirred at room temperature. Then chloromethyl methyl ether (34 mL; 99%) was added slowly, and the mixture was stirred at 55 °C for 24 h. The obtained mixture was precipitated in rigorously stirred methanol. Then the mixture was filtered and the resulting polymer was washed with methanol three times. The obtained CMPSF was dried in vacuum at 50 °C for 24 h. The degree of chloromethylation, obtained by ^{1}H NMR (recorded on a Bruker DRX400 using DMSO-d_6 as the solvent and tetramethylsilane (TMS) as the internal standard, Supporting Information Figure S1) was determined to be 1.72 according to the literature.[26]

Membrane Preparation. The CMPSF-x (x is the ratio of 4,4′-bipyridine to chloromethyl groups of CMPSF) was cast from 20 wt % *N*,*N*-dimethylacetamide (DMAc) solutions and thermally treated at 50 °C for 12 h. The thickness of the prepared membranes was 45 ± 5 μm.

Membrane Characterization. *Water Uptake and Swelling.* Water uptake and swelling of membranes were detected by soaking the membranes in deionized water for 3 days at room temperature. The weight of the saturated membranes was then obtained after quickly wiping off the surface water using a tissue paper. The water uptake was calculated as

$$\text{water uptake} = \frac{W_w - W_d}{W_d} \times 100\%$$

where W_w and W_d are the weights of the saturated and dry membranes, respectively.

The swelling was calculated as

$$\text{swelling} = \frac{L_w - L_d}{L_d} \times 100\%$$

where L_w and L_d are the length of the saturated and dry membranes, respectively.

Ex Situ Oxidation Stability Test. To investigate the influence of ion exchange groups on the chemical stability of the membranes, CMPSF-x membranes with fixed size (5 cm × 5 cm) were soaked in 60 mL of 0.15 M VO_2^+ (3 M H_2SO_4) electrolyte solution in sealed glass vials at 40 °C. A 4 mL electrolyte was collected from each vial at a regular time interval. The concentration of VO^{2+} was determined by a UV−vis spectrometer (JASCO, FT-IR 4100, Japan). To accelerate the degradation process, a more concentrated VO_2^+ solution (1.5 M VO_2^+ in 3 M H_2SO_4) was used to treat the membrane (the immersion time was kept at 18 days, 40 °C). Attenuated total reflection-Fourier transform-infrared (ATR-FT-IR, iS50 FT-IR, Nicolet, Thermo Scientific, recorded at the average rate of 48 scans with a resolution of 4 cm^{-1} collected from 600 to 4000 cm^{-1} in reflection mode) and Raman (Renishaw inVia Raman microscope, 1064 nm, 450 mW) were used to further analyze the degradation products.

In Situ VFB Performance Test. In situ VFB performance test was carried out to investigate the stability of ion exchange groups (by immersing several pieces of 5 cm × 5 cm CMPSF-1.0 membranes in 1.5 M VO_2^+ for different times at 40 °C) and the influence of carbon dioxide on the N-containing membrane (via passing CO_2 gas through different solutions containing CMPSF-1.0 membranes for 1 h and then sealed and held in a water bath at 40 °C for different times). The VFB single cell was assembled by sandwiching a membrane with two carbon felt electrodes, clamped by two polar plates. All these components were fixed between two stainless plates. The effective area of the membrane was 3 cm × 3 cm. A volume of 30 mL of 1.5 M VO^{2+}/VO_2^+ in 3 M H_2SO_4 and 30 mL of 1.5 M V^{2+}/V^{3+} in 3 M H_2SO_4 were used as the positive and negative electrolytes, respectively. The electrolyte was cyclically pumped into the corresponding half-cell. The battery performance tests were conducted using Arbin BT 2000 with a constant current density of 80 mA/cm^2. The battery was charged to an upper limit voltage of 1.65 V and discharge to a lower voltage of 0.8 V, respectively, to avoid the corrosion of the carbon felts and graphite polar plates.

TEM. The distribution of positive charged bipyridine groups in the CMPSF-1.0 membrane was recorded using TEM (JEM-2000EX, JEOL). The membrane sample was treated with 0.02 M palladium chloride solution and then washed with deionized water to remove the palladium ions absorbed in the membrane. After that, the membrane sample was dried and then fixed in epoxy before being cut into thin slice samples.

SEM. The cross-sectional and surface morphologies of the membrane before and after degradation were detected by SEM (JEOL 6360LV, Japan) with an acceleration voltage of 15 kV. The cross sections were obtained by breaking the membranes in liquid nitrogen and coating them with gold prior to imaging.

Stability Test of 4,4′-Bipyridine. To investigate the chemical stability of 4,4′-bipyridine, 0.3230 mmol of 4,4′-bipyridine was soaked in 60 mL of electrolyte solution (0.15 M VO_2^+ in 3 M H_2SO_4) in sealed glass vials at 40 °C. During the test, UV−vis spectroscopic quantification of the reduction process of VO_2^+ to VO^{2+} was recorded as an indication of 4,4′-bipyridine stability.

RESULTS AND DISCUSSION

In this work, polysulfone (PSF) based anion exchange membranes with internal cross-linking networks were prepared via reaction between chloromethylated polysulfone and 4,4′-bypyridine. The 4,4′-bipyridine connects with the CMPSF to establish the internal cross-linking structure and provide ion conductivity, therefore ensuring the high selectivity and stability in a VFB. The chloromethylated polysulfone (CMPSF) contains 1.7 chlorine methyl groups per repeat unit (determined by the ^{1}H NMR, Supporting Information Figure S1), which is the reaction site for further functionalization (Figure 1). The nucleophilic substitution reaction between 4,4′-bipyridine and CMPSF leads to the prepared membranes having both internal cross-linking networks and ion exchange groups. The cross-linking degree and the content of ion

DOI: 10.1021/acsami.5b05840
ACS Appl. Mater. Interfaces 2015, 7, 19446−19454

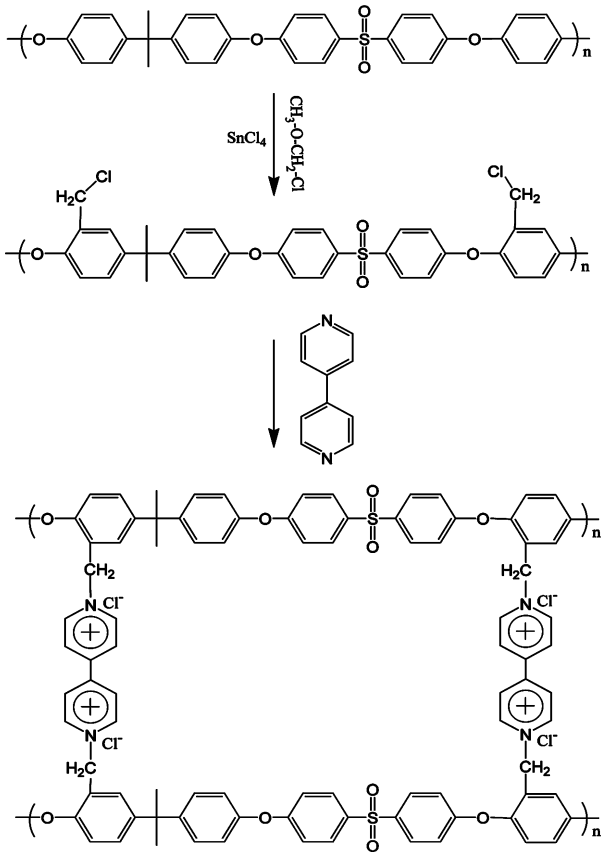

Figure 1. Synthetic scheme for the fabrication of polysulfone based anion exchange membrane.

exchange groups were controlled via changing the content of 4,4′-bipyridine. The membranes prepared from different content of 4,4′-bipyridine were referred as CMPSF-x, where x is the ratio of 4,4′-bipyridine to chloromethyl groups of CMPSF.

Previous studies on cation exchange membranes indicated that the oxidation stability of the membranes is strongly dependent on the amount of ion exchange groups (sulfonic acid functional groups).[27,28] Similarly, attempts to understand the role of ion exchange groups on chemical stability of anion exchange membranes have been investigated by changing the content of 4,4′-bipyridine. Table 1 shows the polysulfone-based

Table 1. Physical Property of Prepared CMPSF Membranes

membrane	chloromethyl group (mmol)	bipyridine (mmol)	water uptake (%)	swelling (%)
CMPSF-0.4	1	0.4	8.62	3.45
CMPSF-0.8	1	0.8	14.8	7.14
CMPSF-1.0	1	1.0	34.85	15.38

anion exchange membranes with different content of 4,4′-bipyridine (ion exchange groups). A clear increase in water uptake and swelling was observed with an increasing content of the bipyridine group. This increase can be attributed to the increased content of hydrophilic pyridine groups in the membranes. Consequently, increasing the content of hydrophilic pyridine groups, which formed hydrophilic water channels, induced higher water uptake and swelling.

To detect the distribution of the ion exchange groups, transmission electron microscope (TEM) analysis was carried out on the initial CMPSF-1.0 membrane after staining by 0.02 M $[PdCl_4]^{2-}$. The dark spots in the membrane (Supporting Information Figure S2) are attributed to the clusters formed by the interaction between negatively $[PdCl_4]^{2-}$ and positively charged 4,4′-bipyridine groups,[11] showing the distribution of 4,4′-bipyridine groups.

As an indicator of membrane stability in electrolytes, the UV−vis spectroscopic quantification of the reduction process of VO_2^+ to VO^{2+}[29] provides an effective and direct way to investigate the influence of ion exchange groups on the chemical stability of the membranes. CMPSF-x membranes with fixed size (4.5 cm × 4.5 cm) and different ion exchange groups (CMPSF-0.4, CMPSF-0.8, CMPSF-1.0) were immersed in 0.15 M VO_2^+ + 3 M H_2SO_4 solutions (40 °C water bath), where an reduction of VO_2^+ as an indicator for membranes oxidation can be readily evaluated as shown in Figure 2. In a

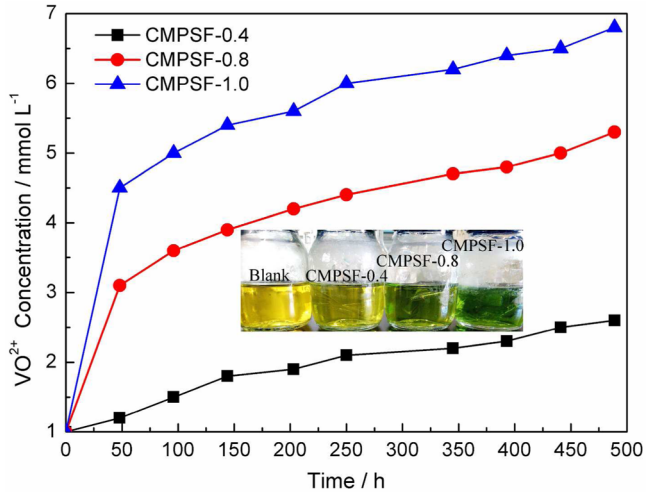

Figure 2. Effect of ion exchange groups (4,4′-bipyridine) on chemical stability of CMPSF membranes (Inserts show the color changes of electrolyte solutions (0.15 M VO_2^+ in 3 M total sulfate) containing CMPSF-0.4, CMPSF-0.8, and CMPSF-1.0 membranes, respectively, after 4 months).

similar vein, obvious color gradients (yellow → green) were detected in 0.15 M VO_2^+ + 3 M H_2SO_4 solutions containing CMPSF-X membranes with different ion exchange groups, suggesting that the similar role of ion exchange groups in the degradation of anion exchange membranes with that of cation exchange ones (ion exchange groups accelerate the degradation of the membranes).[27]

Accelerated degradation experiment was performed to further clarify the degradation mechanism of the anion exchange membranes. As shown in Figure 3a, the CMPSF membrane without 4,4′-bipyridine groups is essentially transparent, while the color of CMPSF-1.0 membrane appears yellow (Figure 3b) as does the color of 4,4′-bipyridine power. After immersing the CMPSF-1.0 membrane in the 1.5 M VO_2^+ + 3 M H_2SO_4 solutions at 40 °C for 18 days, the membrane becomes wine red, which results from the physical absorption of VO_2^+ ions. Instead of color change, the CMPSF-1.0 was broken up as shown in Figure 3c, demonstrating the chemical oxidation of the membrane. Nevertheless, after a few hours of treatment with 3 M H_2SO_4 solutions, the color of the CMPSF-1.0 membrane was observed to revert in yellow (Figure 3d),

DOI: 10.1021/acsami.5b05840
ACS Appl. Mater. Interfaces 2015, 7, 19446−19454

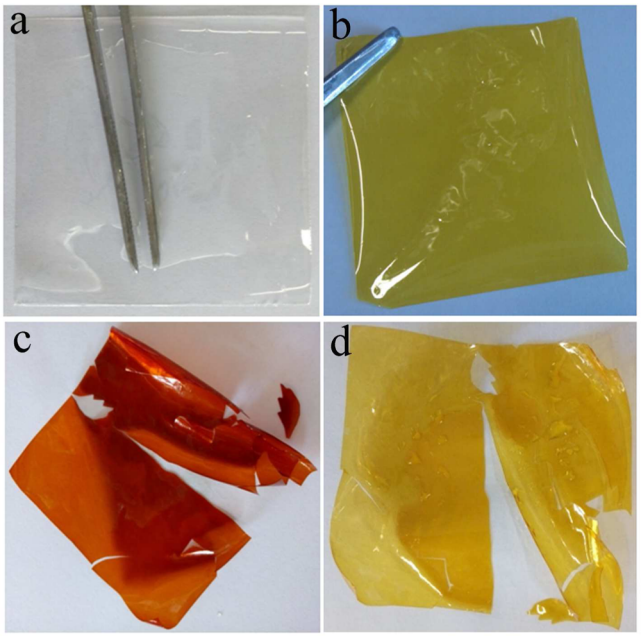

Figure 3. Images of CMPSF membranes: (a) CMPSF, (b) CMPSF-1.0 membrane, (c) CMPSF-1.0 membrane after immersion in 1.5 M VO_2^+ for 18 days, (d) CMPSF-1.0 membrane after immersion in 1.5 M VO_2^+ for 18 days and treated with 3 M H_2SO_4.

which is a very good indication for the stability of the ion exchange groups.

It is well-established for ion exchange membranes that a high concentration of VO_2^+ treatment (immersion in 1.5 M or even more higher concentration of VO_2^+ at 40 °C for a certain period of time) helps to investigate the stability of the membranes, resulting in a dramatic change in battery performance (especially for voltage efficiency when the chemical stability of ion exchange groups was poor). Thus, in situ battery performance was made for CMPSF-1.0 both as prepared and after 1.5 M VO_2^+ treatment (0, 3, 7, and 12 days). The results are shown in Figure 4. The battery performance for all the membranes remains unchanged with increasing immersion time, for both as prepared and 1.5 M VO_2^+ treated

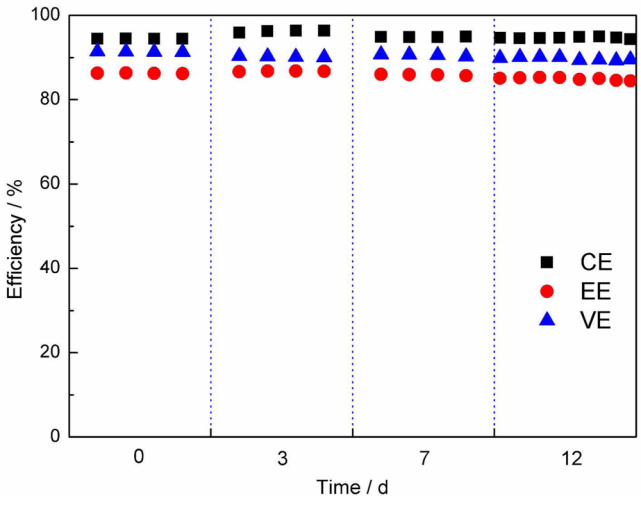

Figure 4. Oxidation stability test of ion exchange groups (4,4′-bipyridine) in 1.5 M VO_2^+ solution.

membranes. This reflects that the 4,4′-bipyridine ion exchange groups in the CMPSF-1.0 membrane exhibits extraordinarily high chemical stability. Note that the aromatic conjugation system remains unspoilt when the pyridinic nitrogen reacts with electrophilic reagent ($-CH_2-Cl$), due to the fact that the lone pair electrons in pyridine nitrogen do not participate in conjugation. As a result, the six membered pyridine ring still has aromaticity even when it is converted to pyridinium salt, which leads to high chemical stability of the pyridine ring.

The morphological characterization of the initial and degraded CMPSF-1.0 membranes was conducted to confirm the formation of micropores in the membrane. In contrast to the initial CMPSF-1.0 membrane, where the surface (Figure 5a) and cross sections (Figure 5b) of the membrane exhibit a

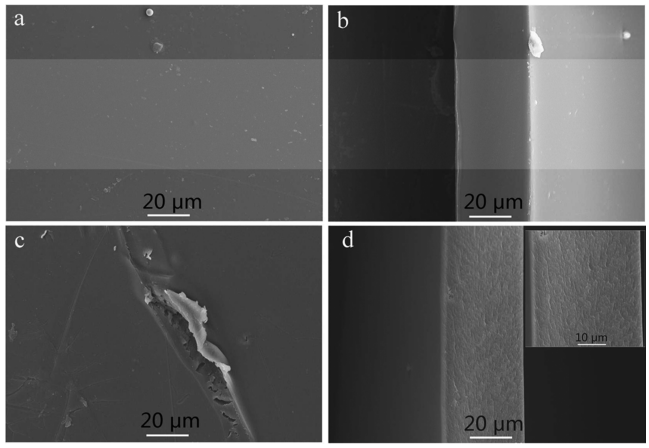

Figure 5. SEM micrographs of CMPSF-1.0 membrane before ((a) surface and (b) cross-section) and after degradation ((c) surface and (d) cross-section). Insert: an enlarged cross-section of degraded CMPSF-1.0 membrane.

smooth and dense structure, however, the degraded membrane was covered with cracks and pores, for both the surface (Figure 5c) and cross section (Figure 5d).

The above discussion has proven that the ion exchange groups, or $-C-N=$ bond in the membrane is chemically stable in VO_2^+ electrolyte. In order to further prove the chemical stability of 4,4′-bipyridine, 0.3230 mmol of 4,4′-bipyridine was immersed in 0.15 M VO_2^+ in 3 M total sulfate at 40 °C. Note that the color of the solution and VO^{2+} concentration detected by UV−vis spectroscopic reflect the stability of 4,4′-bipyridine. As shown in Figure 6, no significant color change could be observed after immersing 0.3230 mmol of 4,4′-bipyridine in 0.15 M VO_2^+ + 3 M total sulfate at 40 °C for 3.5 months. Also, the VO^{2+} concentration in the solution remains constant with increasing immersion time, suggesting the antioxidant capacity of 4,4′-bipyridine. In another word, the ring-opening reaction of the pyridine ring and cracking of the C−C bond between the two pyridine rings could not happen.

Normally, a VFB is operated under ambient conditions, where the interactions between Lewis acid (CO_2 in the air) and Lewis base (N-containing organic heterocyclic molecules, 4,4′-bipyridine in the membrane) may cause the membrane degradation.[18,30] Thus, two CO_2 treatment processes were implemented to investigate the effect of CO_2 on the stability of the CMPSF-1.0 membrane, one is passing CO_2 gas through deionized water that contained a fixed size CMPSF-1.0 membrane for 1 h in sealed glass and the other is passing

DOI: 10.1021/acsami.5b05840
ACS Appl. Mater. Interfaces 2015, 7, 19446−19454

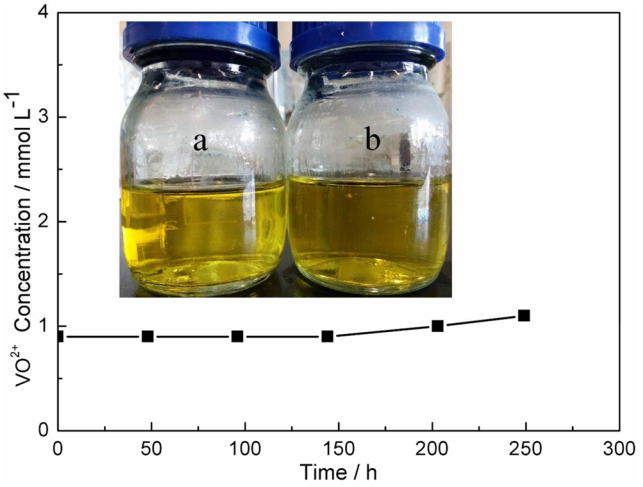

Figure 6. Chemical stability test of 4,4′-bipyridine in 0.15 M VO_2^+ in 3 M total sulfate. Insert: image of 0.15 M VO_2^+ + 3 M total sulfate (a) and 0.15 M VO_2^+ + 3 M total sulfate + 0.3230 mmol of 4,4′-bipyridine after 3.5 months.

CO_2 gas through a 0.15 M VO_2^+ + 3 M total sulfate solution that contained the CMPSF-1.0 membrane for 1 h in another sealed glass. Then the sealed glasses were held in a water bath at 40 °C (5 days for the deionized water glass and 10 days for 0.15 M VO_2^+ + 3 M total sulfate solution glass). As shown in Figure 7, batteries that are assembled with the CMPSF-1.0

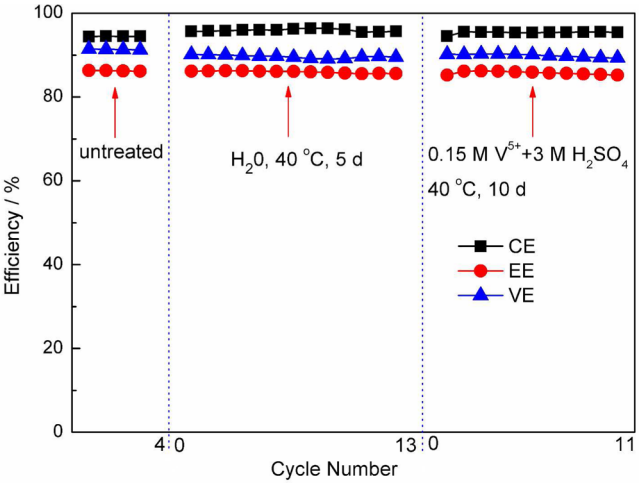

Figure 7. Influence of carbon dioxide on N-containing organic molecule (ion exchange groups).

membranes before and after CO_2 treatment showed stable performance with different cycles, which indicates that the CO_2 will not degrade the membrane as well as the 4,4′-bipyridine groups.

FT-IR spectroscopy was applied to gain further insight into the chemical structure of the degraded CMPSF-1.0 membrane. Figure 8 shows the FT-IR spectra of the initial (black line, corresponding to Figure 3b) and degraded (red line, corresponding to Figure 3d) CMPSF-1.0 membranes. The bands at 1616 and 1579 cm^{-1} in initial and degraded membranes correspond to characteristic frequency of the C═C stretching vibration of the pyridine ring. In addition, the C═N stretching vibration in pyridine ring and inter-ring stretching vibration can be found in 1520 and 1293 cm^{-1} for both initial

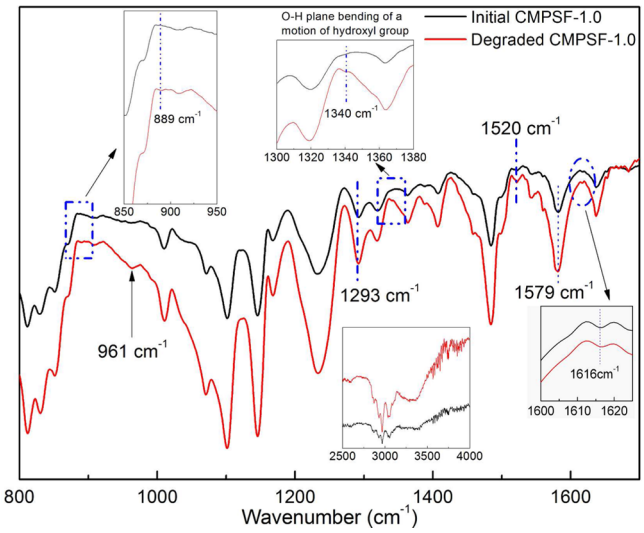

Figure 8. ATR-FT-IR spectra of initial CMPSF-1.0 membrane (black line) and degraded CMPSF-1.0 membrane (red line).

and degraded membranes.[31−33] Some minor changes were clearly observed on the membrane after degradation. For instance, the degraded CMPSF-1.0 membrane exhibits two additional absorption bands at about 889 and 1340 cm^{-1}. The absorption at 889 cm^{-1} was associated with the phenolic hydroxyl group bending vibration.[34] The latter was assigned to O−H plane bending of a motion of hydroxyl group.[35,36] The −OH formation was further supported by the frequency at about 3340 cm^{-1}, which can be ascribed to the stretching modes of the water molecules coordinated to hydroxyl groups via the hydrogen bond interaction.[37] Beyond that, a clear absorption band at about 961 cm^{-1} can be found for the degraded membrane as well, which was considered as characteristic of vanadium oxygen species.[38,39]

Further evidence for the attachment of the vanadium oxygen species to the polymer backbone and the formation of OH after degradation (corresponding to Figure 3d) is shown by Raman experiments (Figure 9). Compared to the initial CMPSF-1.0 membrane, the Raman stretching frequencies of the V−O

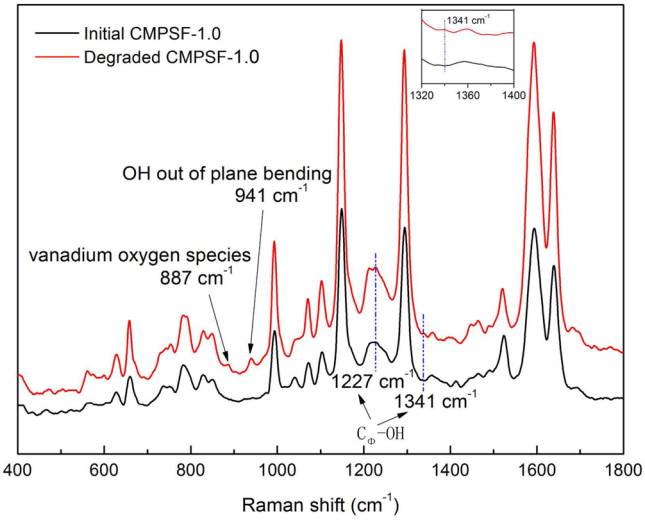

Figure 9. Raman spectra of initial CMPSF-1.0 membrane (black line) and degraded CMPSF-1.0 membrane (red line).

DOI: 10.1021/acsami.5b05840
ACS Appl. Mater. Interfaces 2015, 7, 19446−19454

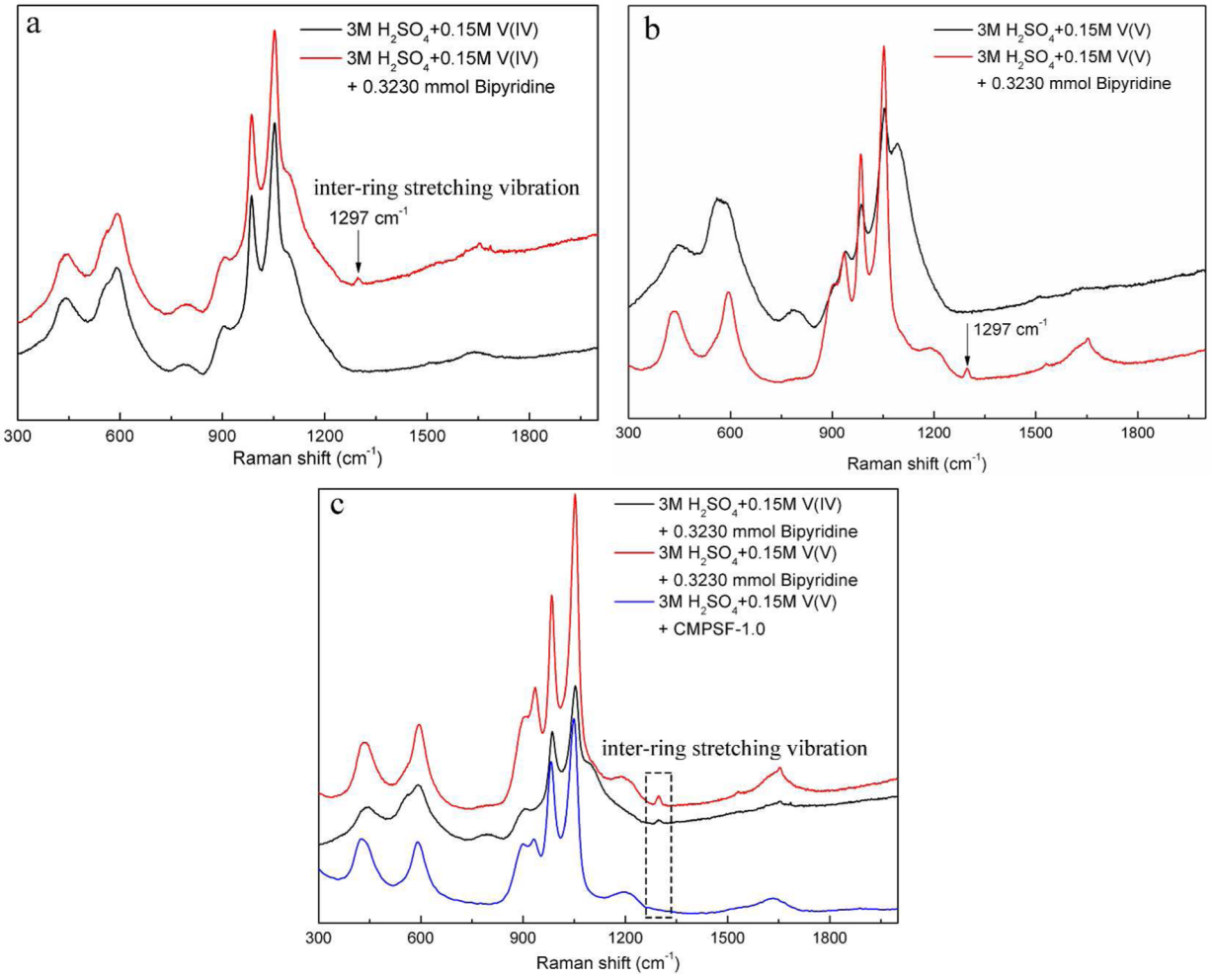

Figure 10. Raman spectra of vanadium solutions (a) 0.15 M VO^{2+} + 3 M H_2SO_4 (black line) and 0.15 M VO^{2+} + 3 M H_2SO_4 + 0.3230 mmol of 4,4′-bipyridine (red line); (b) 0.15 M VO_2^+ + 3 M H_2SO_4 (black line) and 0.15 M VO_2^+ + 3 M H_2SO_4 + 0.3230 mmol of 4,4′-bipyridine (red line); (c) 0.15 M VO^{2+} + 3 M H_2SO_4 + 0.3230 mmol of 4,4′-bipyridine (black line), 0.15 M VO_2^+ + 3 M H_2SO_4 + 0.3230 mmol of 4,4′-bipyridine (red line), and 0.15 M VO_2^+ + 3 M H_2SO_4 + CMPSF-1.0 after 9 months.

vibration for the vanadium oxygen species can be observed at 887 cm^{-1} for the degraded CMPSF-1.0 membrane,[40−43] which suggested again that vanadium oxygen species were incorporated into CMPSF-1.0 after degradation. On the other hand, we assigned the band at 941 cm^{-1} to the OH out of plane bending,[44] and the band at 1341 and 1227 cm^{-1} to the in plane bending model of the phenolic group and in plane bending $C_Φ$−OH ($C_Φ$ is related to the aromatic ring) model, respectively.[45,46] These results are in good agreement with FT-IR results (Figure 8).

In addition, the degraded CMPSF-1.0 membrane was insoluble in most solvents, e.g., DMF, DMAC, DMSO, etc., suggesting that the internal cross-linking networks have not been destroyed. The low solubility of degraded products brings difficulty to identify their chemical structures. On the other hand, there is also the possibility that some degradation products with small molecular weights may be dissolved in the vanadium electrolyte. To confirm this possibility, Raman was performed on the electrolyte solutions (60 mL of 0.15 M VO_2^+ in 3 M total sulfate containing CMPSF-1.0 membrane (Figure 10c), 60 mL of 0.15 M VO_2^+ in 3 M total sulfate with and without 0.3230 mmol of 4,4′-bipyridine (Figure 10b), and 60 mL of 0.15 M VO^{2+} in 3 M total sulfate with and without 0.3230 mmol of 4,4′-bipyridine (Figure 10a), held in a water bath at 40 °C for 9 months. The test time is long enough to degrade the membrane into shorter chains. Note that the paramagnetic VO^{2+} allows that ^1H NMR can perform neither on the VO^{2+} solution nor the VO^{2+}/VO_2^+ mixture. Figure 10 shows the Raman spectra of electrolyte samples after treatment. After the addition of 0.3230 mmol of 4,4′-bipyridine in the VO^{2+} and VO_2^+ ion containing electrolytes, only inter-ring stretching vibration at 1297 cm^{-1} can be observed as compared with both VO^{2+} and VO_2^+ ions containing electrolytes that did not contain any 4,4′-bipyridine (Figure 10a,b), whereas the spectra of CMPSF-1.0 membrane containing electrolyte shows no significant characteristic absorption bands for any organics (Figure 10c) as well, revealing that no degradation products with small molecular weights in the vanadium electrolytes were observed.

On the basis of the above results, a possible mechanism for the degradation of polysulfone based anion exchange membrane is shown in Figure 11. The electron-donating alkyl group and the weak electron withdrawing chloromethyl group along with protonated ether functionality balance the charge state of pristine chloromethylated polysulfone and, thus, maintain the high chemical stability of CMPSF in strong oxidizing electrolyte. While in the case of CMPSF-x, this charge state was disrupted by the nucleophilic substitution reaction,

DOI: 10.1021/acsami.5b05840
ACS Appl. Mater. Interfaces 2015, 7, 19446−19454

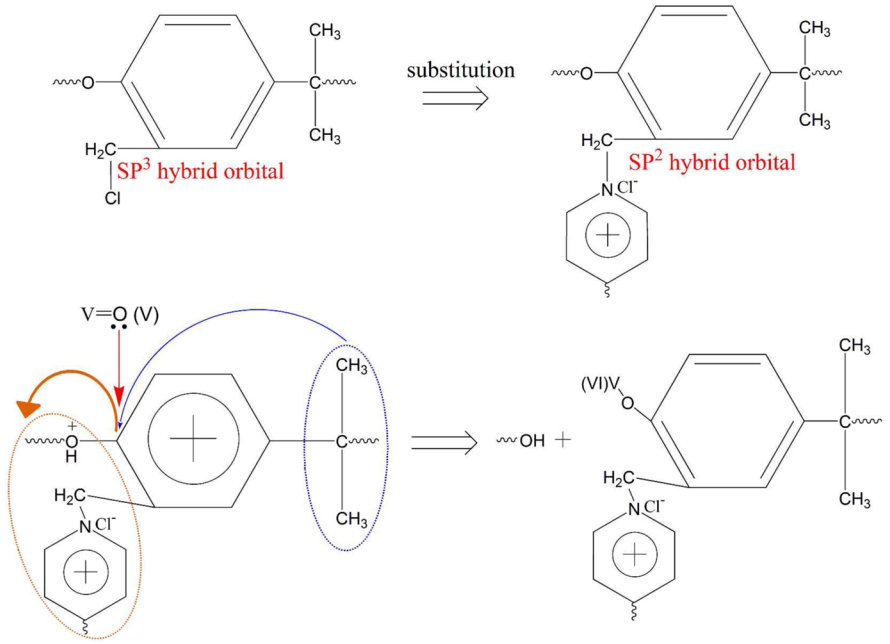

Figure 11. Proposed degradation mechanism of polysulfone based anion exchange membranes (carrying 4,4′-bipyridine ion exchange groups) during the ex situ oxidation stability test.

which is caused by the fracture of the C−Cl bond (formed by the sp^3 hybrid orbital of carbon and the sp^3 hybrid orbital of chlorine) and the formation of the C−N bond (realized by the sp^2 hybrid orbital in pyridinic-nitrogen in 4,4′-bipyridine). Compare the sp^3 hybrid orbital to the sp^2 hybrid orbital, the sp^2 hybrid orbital turns out to be more electronegative, resulting from more s ingredient in the sp^2 hybrid orbital.[47] This difference in electronegativity induces an electrophilic carbon center on the benzene ring, which can be attacked by the lone pair electron on the vanadium(V) oxygen species, with the formation of a phenolic hydroxyl group and vanadium(IV) oxygen species as shown in Figure 8 and Figure 9. In fuel cells, it is generally believed that the chemical stability of the membrane was highly dependent on the nature of the functional group, and a stable cation moiety is sufficient to yield a stable membrane.[48−53] Thus, the issue of backbone stability was often ignored. According to the proposed mechanism, the CMPSF-1.0 membrane may also be attacked by the hydroxide ions, further leading to backbone degradation. Therefore, the importance of polymer backbone stability should also be emphasized under battery operating medium.

To support the mechanism we proposed above, CMPSF-1.0 membranes were immersed in 0.15 M VO_2^+ solutions with increasing concentrations of sulfuric acid (1, 2, and 3 M) and also corresponding to an increase in the electronegativity of the polymer backbone (resulting from the protonation of the ethereal oxygen atoms) to confirm the influence of electronegativity on the stability of the membrane since the electronic effect of alkyl group and 4,4′-bipyridine is regular. As expected, the concentration of VO^{2+} reduced from VO_2^+ increases with increasing acid concentration and also corresponds to more serious degradation, further confirming our assumptions (Supporting Information Figure S3).

CONCLUSIONS

In summary, we have investigated the degradation mechanism of the polysulfone based anion exchange membranes under VFB medium for the first time. The results showed that, as a result of substitution of SP^2 hybrid orbital interactions between C−N bond for SP^3 hybrid orbital interactions between C−Cl bond, the charge state balance of pristine chloromethylated polysulfone is likely to be disrupted. Further, this substitution is closely associated with corresponding changes in electronegativity and thus inducing an electrophilic carbon center in the benzene ring. The electrophilic carbon center can be attacked by the lone pair electron on the vanadium(V) oxygen species and will result in brittle membranes. Therefore, strategies such as introducing electron-donating groups to the aromatic backbone, protecting the ether bond, or using pendant groups to separate the ion exchange groups from the polymer backbone may be effective ways to improve the stability of membranes.

ASSOCIATED CONTENT

Supporting Information

The Supporting Information is available free of charge on the ACS Publications website at DOI: 10.1021/acsami.5b05840.

NMR spectra of CMPSF, TEM image of CMPSF-1.0 membrane, and UV−vis data (PDF)

AUTHOR INFORMATION

Corresponding Authors

*E-mail: lixianfeng@dicp.ac.cn.
*E-mail: zhanghm@dicp.ac.cn.

Notes

The authors declare no competing financial interest.

ACKNOWLEDGMENTS

The authors greatly acknowledge the financial support from China Natural Science Foundation (Grant Nos. 21206158, 21476224, and 51361135701), the Outstanding Young Scientist Foundation, Chinese Academy of Sciences (CAS), the Key Research Program of the Chinese Academy of Sciences

DOI: 10.1021/acsami.5b05840
ACS Appl. Mater. Interfaces 2015, 7, 19446−19454

(Grant KG2D-EW-602-2), Science and Technology Service Network Initiative (Grant KFJ-EW-STS-108), and Dalian Municipal Outstanding Young Talent Foundation (Grant 2014J11JH131).

REFERENCES

(1) Bouchet, R.; Maria, S.; Meziane, R.; Aboulaich, A.; Lienafa, L.; Bonnet, J.-P.; Phan, T. N.; Bertin, D.; Gigmes, D.; Devaux, D. Single-Ion BAB Triblock Copolymers as Highly Efficient Electrolytes for Lithium-Metal Batteries. *Nat. Mater.* **2013**, *12*, 452−457.

(2) Dunn, B.; Kamath, H.; Tarascon, J.-M. Electrical Energy Storage for the Grid: A Battery of Choices. *Science* **2011**, *334*, 928−935.

(3) Ji, X.; Lee, K. T.; Nazar, L. F. A Highly Ordered Nanostructured Carbon−Sulphur Cathode for Lithium−Sulphur Batteries. *Nat. Mater.* **2009**, *8*, 500−506.

(4) Wang, W.; Luo, Q.; Li, B.; Wei, X.; Li, L.; Yang, Z. Recent Progress in Redox Flow Battery Research and Development. *Adv. Funct. Mater.* **2013**, *23*, 970−986.

(5) Yang, Z.; Zhang, J.; Kintner-Meyer, M. C.; Lu, X.; Choi, D.; Lemmon, J. P.; Liu, J. Electrochemical Energy Storage for Green Grid. *Chem. Rev.* **2011**, *111*, 3577−3613.

(6) Li, X.; Zhang, H.; Mai, Z.; Zhang, H.; Vankelecom, I. Ion Exchange Membranes for Vanadium Redox Flow Battery (VRB) Applications. *Energy Environ. Sci.* **2011**, *4*, 1147−1160.

(7) Li, N.; Guiver, M. D. Ion Transport by Nanochannels in Ion-Containing Aromatic Copolymers. *Macromolecules* **2014**, *47*, 2175−2198.

(8) Mauritz, K. A.; Moore, R. B. State of Understanding of Nafion. *Chem. Rev.* **2004**, *104*, 4535−4586.

(9) Mai, Z.; Zhang, H.; Zhang, H.; Xu, W.; Wei, W.; Na, H.; Li, X. Anion-Conductive Membranes with Ultralow Vanadium Permeability and Excellent Performance in Vanadium Flow Batteries. *ChemSusChem* **2013**, *6*, 328−335.

(10) Zhang, S.; Yin, C.; Xing, D.; Yang, D.; Jian, X. Preparation of Chloromethylated/Quaternized Poly (Phthalazinone Ether Ketone) Anion Exchange Membrane Materials for Vanadium Redox Flow Battery Applications. *J. Membr. Sci.* **2010**, *363*, 243−249.

(11) Bae, B.; Yoda, T.; Miyatake, K.; Uchida, H.; Watanabe, M. Proton-Conductive Aromatic Ionomers Containing Highly Sulfonated Blocks for High-Temperature-Operable Fuel Cells. *Angew. Chem.* **2010**, *122*, 327−330.

(12) Roziere, J.; Jones, D. J. Non-fluorinated Polymer Materials for Proton Exchange Membrane Fuel Cells. *Annu. Rev. Mater. Res.* **2003**, *33*, 503−555.

(13) Guo, X.; Fang, J.; Watari, T.; Tanaka, K.; Kita, H.; Okamoto, K.-i. Novel Sulfonated Polyimides as Polyelectrolytes for Fuel Cell Application. 2. Synthesis and Proton Conductivity of Polyimides from 9, 9-Bis (4-aminophenyl) Fluorene-2, 7-Disulfonic Acid. *Macromolecules* **2002**, *35*, 6707−6713.

(14) Ding, C.; Zhang, H.; Li, X.; Liu, T.; Xing, F. Vanadium Flow Battery for Energy Storage: Prospects and Challenges. *J. Phys. Chem. Lett.* **2013**, *4*, 1281−1294.

(15) Jung, M.-S. J.; Parrondo, J.; Arges, C. G.; Ramani, V. Polysulfone-Based Anion Exchange Membranes Demonstrate Excellent Chemical Stability and Performance for the All-Vanadium Redox Flow Battery. *J. Mater. Chem. A* **2013**, *1*, 10458−10464.

(16) Merle, G.; Wessling, M.; Nijmeijer, K. Anion Exchange Membranes for Alkaline Fuel Cells: A Review. *J. Membr. Sci.* **2011**, *377*, 1−35.

(17) Couture, G.; Alaaeddine, A.; Boschet, F.; Ameduri, B. Polymeric Materials as Anion-Exchange Membranes for Alkaline Fuel Cells. *Prog. Polym. Sci.* **2011**, *36*, 1521−1557.

(18) Varcoe, J. R.; Atanassov, P.; Dekel, D. R.; Herring, A. M.; Hickner, M. A.; Kohl, P. A.; Kucernak, A. R.; Mustain, W. E.; Nijmeijer, K.; Scott, K. Anion-Exchange Membranes in Electrochemical Energy Systems. *Energy Environ. Sci.* **2014**, *7*, 3135−3191.

(19) Deavin, O. I.; Murphy, S.; Ong, A. L.; Poynton, S. D.; Zeng, R.; Herman, H.; Varcoe, J. R. Anion-Exchange Membranes for Alkaline Polymer Electrolyte Fuel Cells: Comparison of Pendent Benzyltrimethylammonium-and Benzylmethylimidazolium-Head-Groups. *Energy Environ. Sci.* **2012**, *5*, 8584−8597.

(20) Yu, T. H.; Sha, Y.; Liu, W.-G.; Merinov, B. V.; Shirvanian, P.; Goddard, W. A., III Mechanism for Degradation of Nafion in PEM Fuel Cells from Quantum Mechanics Calculations. *J. Am. Chem. Soc.* **2011**, *133*, 19857−19863.

(21) Arges, C. G.; Ramani, V. Two-Dimensional NMR Spectroscopy Reveals Cation-Triggered Backbone Degradation in Polysulfone-Based Anion Exchange Membranes. *Proc. Natl. Acad. Sci. U. S. A.* **2013**, *110*, 2490−2495.

(22) Chempath, S.; Boncella, J. M.; Pratt, L. R.; Henson, N.; Pivovar, B. S. Density Functional Theory Study of Degradation of Tetraalkylammonium Hydroxides. *J. Phys. Chem. C* **2010**, *114*, 11977−11983.

(23) Xu, W.; Zhao, Y.; Yuan, Z.; Li, X.; Zhang, H.; Vankelecom, I. F. J. Highly Stable Anion Exchange Membranes with Internal Cross-Linking Networks. *Adv. Funct. Mater.* **2015**, *25*, 2583−2589.

(24) Wei, X.; Nie, Z.; Luo, Q.; Li, B.; Chen, B.; Simmons, K.; Sprenkle, V.; Wang, W. Nanoporous Polytetrafluoroethylene/Silica Composite Separator as a High-Performance All-Vanadium Redox Flow Battery Membrane. *Adv. Energy Mater.* **2013**, *3*, 1215−1220.

(25) Zhang, F.; Zhang, H.; Qu, C. A Dication Cross-Linked Composite Anion-Exchange Membrane for All-Vanadium Flow Battery Applications. *ChemSusChem* **2013**, *6*, 2290−2298.

(26) Parrondo, J.; Arges, C. G.; Niedzwiecki, M.; Anderson, E. B.; Ayers, K. E.; Ramani, V. Degradation of Anion Exchange Membranes Used for Hydrogen Production by Ultrapure Water Electrolysis. *RSC Adv.* **2014**, *4*, 9875−9879.

(27) Yuan, Z.; Li, X.; Hu, J.; Xu, W.; Cao, J.; Zhang, H. Degradation Mechanism of Sulfonated Poly (Ether Ether Ketone) (SPEEK) Ion Exchange Membranes under Vanadium Flow Battery Medium. *Phys. Chem. Chem. Phys.* **2014**, *16*, 19841−19847.

(28) Fujimoto, C.; Kim, S.; Stains, R.; Wei, X.; Li, L.; Yang, Z. G. Vanadium Redox Flow Battery Efficiency and Durability Studies of Sulfonated Diels Alder Poly(phenylene)s. *Electrochem. Commun.* **2012**, *20*, 48−51.

(29) Mohammadi, T.; Kazacos, M. S. Evaluation of the Chemical Stability of Some Membranes in Vanadium Solution. *J. Appl. Electrochem.* **1997**, *27*, 153−160.

(30) Du, N.; Park, H. B.; Robertson, G. P.; Dal-Cin, M. M.; Visser, T.; Scoles, L.; Guiver, M. D. Polymer Nanosieve Membranes for CO2-Capture Applications. *Nat. Mater.* **2011**, *10*, 372−375.

(31) Sen, S.; Mitra, S.; Kundu, P.; Saha, M. K.; Krüger, C.; Bruckmann, J. Synthesis, Characterization and Structural Studies of Mono-and Polynuclear Complexes of Zinc (II) with 1, 10-Phenanthroline, 2, 2′-Bipyridine and 4, 4′-Bipyridine. *Polyhedron* **1997**, *16*, 2475−2481.

(32) Metz, J.; Schneider, O.; Hanack, M. Infrared and Far Infrared Studies of Monomeric and Polymeric Base Adducts of Phthalocyaninato Transition Metal (II) Complexes. *Spectrochim. Acta, Part A: Molecular Spectroscopy* **1982**, *38*, 1265−1273.

(33) Popov, A. I.; Marshall, J. C.; Stute, F. B.; Person, W. B. Studies on the Chemistry of Halogens and of Polyhalides. XXI. Halogen Complexes of 4, 4′-Bipyridine and the Infrared Spectra of Pyridine Complexes. *J. Am. Chem. Soc.* **1961**, *83*, 3586−3590.

(34) Hamann, S. D.; Linton, M. The Influence of Pressure on the Infrared Spectra of Hydrogen-Bonded Solids. I. Compounds with OH-O Bonds. *Aust. J. Chem.* **1975**, *28*, 2567−2578.

(35) Karabacak, M.; Kurt, M. The Spectroscopic (FT-IR and FT-Raman) and Theoretical Studies of 5-Bromo-Salicylic Acid. *J. Mol. Struct.* **2009**, *919*, 215−222.

(36) Nogueira, H. I. Surface-Enhanced Raman Scattering (SERS) of 3-Aminosalicylic and 2-Mercaptonicotinic Acids in Silver Colloids. *Spectrochim. Acta, Part A* **1998**, *54*, 1461−1470.

(37) Tan, K.; Zuluaga, S.; Gong, Q.; Canepa, P.; Wang, H.; Li, J.; Chabal, Y. J.; Thonhauser, T. Water Reaction Mechanism in Metal Organic Frameworks with Coordinatively Unsaturated Metal Ions: MOF-74. *Chem. Mater.* **2014**, *26*, 6886−6895.

DOI: 10.1021/acsami.5b05840
ACS Appl. Mater. Interfaces 2015, 7, 19446−19454

(38) Zhou, M.; Dong, J.; Zhang, L.; Qin, Q. Reactions of Group V Metal Atoms with Water Molecules. Matrix Isolation FTIR and Quantum Chemical Studies. *J. Am. Chem. Soc.* **2001**, *123*, 135−141.
(39) Liu, P.; Moudrakovski, I. L.; Liu, J.; Sayari, A. Mesostructured Vanadium Oxide Containing Dodecylamine. *Chem. Mater.* **1997**, *9*, 2513−2520.
(40) Ding, C.; Ni, X.; Li, X.; Xi, X.; Han, X.; Bao, X.; Zhang, H. Effects of Phosphate Additives on the Stability of Positive Electrolytes for Vanadium Flow Batteries. *Electrochim. Acta* **2015**, *164*, 307−314.
(41) Moura, M.; Ayala, A.; Guedes, I.; Grimsditch, M.; Loong, C.-K.; Boatner, L. Raman Scattering Study of Tb (V 1-x P x) O 4 Single Crystals. *J. Appl. Phys.* **2004**, *95*, 1148−1151.
(42) Kausar, N.; Howe, R.; Skyllas-Kazacos, M. Raman Spectroscopy Studies of Concentrated Vanadium Redox Battery Positive Electrolytes. *J. Appl. Electrochem.* **2001**, *31*, 1327−1332.
(43) Hardcastle, F. D.; Wachs, I. E. Determination of Vanadium-Oxygen Bond Distances and Bond Orders by Raman Spectroscopy. *J. Phys. Chem.* **1991**, *95*, 5031−5041.
(44) Mary, Y. S.; Ushakumari, L.; Harikumar, B.; Varghese, H. T.; Panicker, C. Y. FT-IR, FT-Raman and SERS Spectra of L-Proline. *J. Iran. Chem. Soc.* **2009**, *6*, 138−144.
(45) Humbert, B.; Alnot, M.; Quiles, F. Infrared and Raman Spectroscopical Studies of Salicylic and Salicylate Derivatives in Aqueous Solution. *Spectrochim. Acta, Part A* **1998**, *54*, 465−476.
(46) Tejedor-Tejedor, M. I.; Yost, E. C.; Anderson, M. A. Characterization of Benzoic and Phenolic Complexes at the Goethite/Aqueous Solution Interface Using Cylindrical Internal Reflection Fourier Transform Infrared Spectroscopy. Part 1. Methodology. *Langmuir* **1990**, *6*, 979−987.
(47) Allen, L. C. Electronegativity Is the Average One-Electron Energy of the Valence-Shell Electrons in Ground-State Free Atoms. *J. Am. Chem. Soc.* **1989**, *111*, 9003−9014.
(48) Li, Y.; Zhao, T. Understanding the Performance Degradation of Anion-Exchange Membrane Direct Ethanol Fuel Cells. *Int. J. Hydrogen Energy* **2012**, *37*, 4413−4421.
(49) Chempath, S.; Einsla, B. R.; Pratt, L. R.; Macomber, C. S.; Boncella, J. M.; Rau, J. A.; Pivovar, B. S. Mechanism of Tetraalkylammonium Headgroup Degradation in Alkaline Fuel Cell Membranes. *J. Phys. Chem. C* **2008**, *112*, 3179−3182.
(50) Fang, J.; Shen, P. K. Quaternized Poly (Phthalazinon Ether Sulfone Ketone) Membrane for Anion Exchange Membrane Fuel Cells. *J. Membr. Sci.* **2006**, *285*, 317−322.
(51) Varcoe, J. R.; Slade, R. C. Prospects for Alkaline Anion-Exchange Membranes in Low Temperature Fuel Cells. *Fuel Cells* **2005**, *5*, 187−200.
(52) Komkova, E.; Stamatialis, D.; Strathmann, H.; Wessling, M. Anion-Exchange Membranes Containing Diamines: Preparation and Stability in Alkaline Solution. *J. Membr. Sci.* **2004**, *244*, 25−34.
(53) LaConti, A.; Hamdan, M.; McDonald, R. Fuel Cell Technology and Applications, Polymer Electrolyte Membrane Fuel Cells and Systems (PEMFC), State-of-the-Art Performance and Durability. *Handbook of Fuel Cells* **2003**, DOI: 10.1002/9780470974001.f303055.

DOI: 10.1021/acsami.5b05840
ACS Appl. Mater. Interfaces 2015, 7, 19446−19454